Title

The importance of the shape of cloud droplet size distributions in shallow cumulus clouds. Part I: Bin microphysics simulations

Journal

Journal of the Atmospheric Sciences, 74(1)

ISSN

0022-4928

Authors

Igel, AL
van den Heever, SC

Publication Date

2017

DOI

10.1175/JAS-D-15-0382.1

Peer reviewed

The Importance of the Shape of Cloud Droplet Size Distributions in Shallow Cumulus Clouds. Part I: Bin Microphysics Simulations

ADELE L. IGEL AND SUSAN C. VAN DEN HEEVER

Colorado State University, Fort Collins, Colorado

(Manuscript received 23 December 2015, in final form 12 September 2016)

ABSTRACT

In this two-part study, the relationships between the width of the cloud droplet size distribution and the microphysical processes and cloud characteristics of nonprecipitating shallow cumulus clouds are investigated using large-eddy simulations. In Part I, simulations are run with a bin microphysics scheme and the relative widths (standard deviation divided by mean diameter) of the simulated cloud droplet size distributions are calculated. They reveal that the value of the relative width is higher and less variable in the subsaturated regions of the cloud than in the supersaturated regions owing to both the evaporation process itself and enhanced mixing and entrainment of environmental air. Unlike in some previous studies, the relative width is not found to depend strongly on the initial aerosol concentration or mean droplet concentration. Nonetheless, local values of the relative width are found to positively correlate with local values of the droplet concentrations, particularly in the supersaturated regions of clouds. In general, the distributions become narrower as the local droplet concentration increases, which is consistent with the difference in relative width between the supersaturated and subsaturated cloud regions and with physically based expectations. Traditional parameterizations for the relative width (or shape parameter, a related quantity) of cloud droplet size distributions in bulk microphysics schemes are based on cloud mean values, but the bin simulation results shown here demonstrate that more appropriate parameterizations should be based on the relationship between the local values of the relative width and the cloud droplet concentration.

1. Introduction

Microphysical schemes used in numerical cloud, weather, and climate models usually need to assume a probability distribution to describe the size distribution of each hydrometeor species that is represented by the model. Such schemes are referred to as bulk microphysics schemes. The two distributions that are most commonly used within such schemes are the exponential and gamma probability distributions. Following Walko et al. (1995), the gamma probability distribution function $[n(D)]$ is expressed as

$$n(D) = \frac{N_t}{D_n^{\nu}\Gamma(\nu)} D^{\nu-1} e^{-D/D_n}, \tag{1}$$

where N_t is the total number concentration of the hydrometeor species, D is the species diameter, D_n is called the characteristic diameter, and ν is referred to as the shape parameter. (While not used here, note that the shape parameter may be expressed alternatively as $\mu = \nu - 1$ and a slope parameter may be defined as $\Lambda = 1/D_n$.) The gamma distribution reduces to the exponential distribution when $\nu = 1$. The shape parameter influences the width of the size distribution and can be directly related to the relative dispersion (ε, the ratio of the standard deviation of cloud droplet size to the mean cloud droplet size) of the distribution by $\nu = 1/\varepsilon^2$ (e.g., Hsieh et al. 2009a). For a given mass mean diameter, higher shape parameters (lower relative dispersions) correspond to narrower size distributions that have fewer small and fewer large droplets but more medium sized droplets compared to distributions with lower shape parameters (higher relative dispersions).

To fully describe the gamma distribution given by Eq. (1), three parameters must be known: N_t, D_n, and ν. In two-moment bulk microphysics schemes, N_t and q, the mass mixing ratio of the species are explicitly predicted by the model. Furthermore, for spherical water droplets, D_n and ν can be shown to be related to N_t and q through the relationship

Corresponding author address: Adele L. Igel, Department of Land, Air and Water Resources, University of California, Davis, One Shields Avenue, Davis, CA 95616.
E-mail: aigel@ucdavis.edu

DOI: 10.1175/JAS-D-15-0382.1

TABLE 1. Previously reported values of the shape parameter. In some studies, only the relative dispersion is reported, in which case, we have converted these values to shape parameter values. The notes column describes where the data come from and the meanings of the values in parentheses.

Paper	Campaign	Cloud droplet concentration ($\#\,cm^{-3}$)	Shape parameter	Notes
Costa et al. (2000)	Cearà experiment (Brazil)	227 (maritime)	13.5 (19.3)	Mean (standard deviation). See their Tables 3 and 6.
		265 (coastal)	10.7 (13.5)	
		375 (continental)	12.5 (10.6)	
		433 (urban)	9.8 (10.2)	
Gonçalves et al. (2008)	Dry-to-Wet campaign (Brazil)	521 (clean)	1.9 (1.3)	Mean (standard deviation) of single flights; see their Table 2.
		816 (intermediary)	3.8 (1.2)	
		1451 (polluted)	6.1 (0.7)	
Lu et al. (2008)	GoMACCS (Texas)[a]	206	9.6	Data in their Table 2 split into equal groups based on droplet concentration and averaged.
		282	13.2	
		350	10.9	
Hsieh et al. (2009a)	CRYSTAL-FACE (Florida)[b]	480	5.9 (4.5–8.7)	Mean (25th–75th percentiles). See their Table 1.
	CSTRIPE (California coast)[c]	304	3.2 (2.4–4.5)	
Martins and Silva Dias (2009)	LBA (Brazil)[d]	550	4.3	Data in their Table 1 split into equal groups based on droplet concentration and averaged.
		748	5.7	
		1021	5.3	
Hudson et al. (2012)	RICO (Caribbean)[e]	75	7.1	Their Table 2 flight average (row second from bottom).
Pandithurai et al. (2012)	CAIPEEX-I (India)[f]	264	8.6	Data in their Table 1 split into equal groups based on droplet concentration and averaged.
		326	8.1	
		508	7.3	

[a] Gulf of Mexico Atmospheric Composition and Climate Study.
[b] Cirrus Regional Study of Tropical Anvils and Cirrus Layers—Florida-Area Cirrus Experiment.
[c] Coastal Stratocumulus Imposed Perturbation Experiment.
[d] Large-Scale Biosphere–Atmosphere Experiment.
[e] Rain in Cumulus over the Ocean.
[f] Cloud Aerosol Interaction and Precipitation Enhancement Experiment.

$$q = (N_t \pi / 6 \rho_w D_n^3) \frac{\Gamma(\nu + 3)}{\Gamma(\nu)}, \tag{2}$$

where ρ_w is the density of liquid water. With this relationship, D_n can be solved for if ν is known. However, in single- and double-moment bulk microphysics schemes, ν is not known, and must be set to some constant value or diagnosed in some other way (Grabowski 1998; Rotstayn and Liu 2003; Morrison and Grabowski 2007; Thompson et al. 2008; Geoffroy et al. 2010). On the other hand, triple-moment schemes (Milbrandt and Yau 2005b; Shipway and Hill 2012; Loftus and Cotton 2014), which additionally predict the sixth moment of the distribution, can explicitly solve for this remaining parameter of the gamma distribution. This is the primary advantage of these schemes over lower-moment microphysics schemes, although they are computationally more expensive.

There have been efforts to determine the most appropriate value of the shape parameter from observations of cloud droplet distributions. Table 1 shows a summary of estimates of this parameter for cloud droplets from several recent field measurements of just one cloud type: shallow cumulus clouds. Estimated values range from about 2 to 14. There do not appear to be any consistent differences based on region or surface type (land vs ocean). An even wider range of values was found by Miles et al. (2000), who reported primarily on stratus and stratocumulus clouds. Furthermore, the studies in Table 1, which include clouds sampled in different amounts of air pollution, do not agree on whether the shape parameter should increase or decrease with increasing cloud droplet number concentration. Two studies find an increase (Gonçalves et al. 2008; Martins et al. 2009), two find a decrease (Costa et al. 2000; Pandithurai et al. 2012), and one finds a nonmonotonic change (Lu et al. 2008). There are many potential reasons for these discrepancies ranging from differences in the boundary layer environment to sampling and analysis methods. Regardless, Table 1 indicates that the shape parameter for the cloud droplet size distribution is poorly constrained by observations.

Other investigators have sought to understand the relative dispersion, and thus also the shape parameter, from a

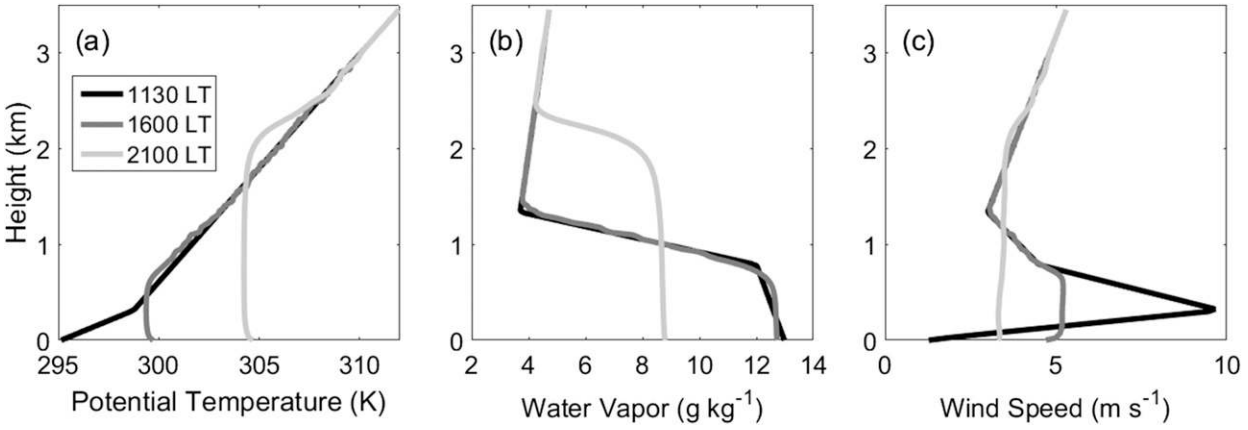

FIG. 1. (a) Potential temperature, (b) water vapor mass mixing ratio, and (c) horizontal wind speed shown every 3 h. The times listed in the legend are local times and the conditions at 1130 LT are the model initial conditions.

theoretical perspective and through modeling studies using bin microphysics schemes, which, by design, preclude the need for an assumed size distribution function (Khain et al. 2015). Processes such as collision–coalescence and entrainment generally widen the distribution (decrease the shape parameter) (Paluch and Baumgardner 1989; Politovich 1993; Feingold et al. 1997; Lu and Seinfeld 2006; Pinsky et al. 2016), whereas condensation will narrow the distribution (increase the shape parameter) (Yum and Hudson 2005; Liu et al. 2006; Peng et al. 2007; Hsieh et al. 2009b; Wang et al. 2011). When only considering condensation, theoretical arguments and parcel modeling have shown that the distribution narrows less (shape parameter increases less) for distributions with initially higher cloud droplet or aerosol concentrations (Yum and Hudson 2005; Liu et al. 2006; Peng et al. 2007; Pinsky et al. 2014). In turn, the shape of the droplet distribution can influence the rate at which these processes act (e.g., Milbrandt and Yau 2005a; Cohen and McCaul 2006). For example, a higher shape parameter (narrower distribution) is expected to result in slower collection of cloud water by rain (Cohen and McCaul 2006) and reduced size sorting for precipitating hydrometeors (Milbrandt and Yau 2005a).

To further understand this complex issue, we will examine simulations of nonprecipitating shallow cumulus clouds in which the only major microphysical processes are droplet nucleation, condensation, and evaporation. These simple clouds are chosen for study in order to isolate the impacts of condensation and evaporation from other microphysical processes as much as possible. In Part I, simulations with a spectral bin microphysics scheme (in which by design the droplet size distribution width evolves with time) will be used to investigate the behavior of the shape parameter in nonprecipitating shallow cumulus clouds and to gain some insight into how microphysical processes impact the shape parameter and how these impacts are modulated by the cloud droplet number concentration. The bin scheme results will be used to guide simulations with a bulk microphysics scheme in Igel and van den Heever (2016, hereafter Part II) in order to investigate how the shape parameter in turn impacts the condensation/evaporation rates and cloud properties in these shallow cumulus clouds.

2. Methods

In this study, the Regional Atmospheric Modeling System (RAMS; Cotton et al. 2003) was used to run simulations of shallow cumulus clouds over land. Semi-idealized thermodynamic profiles (Zhu and Albrecht 2003) from the Atmospheric Radiation Measurement (ARM) Southern Great Plains (SGP) site in Oklahoma were used to initialize the model horizontally homogeneously at 1130 local time (Fig. 1). The model domain was 12.8 km × 12.8 km × 3.5 km with 50-m grid spacing in the horizontal and 25-m grid spacing in the vertical, and the simulations were run for 9.5 h with a 1-s time step. Lateral boundary conditions were periodic and a damping layer was placed in the upper 500 m of the domain. A subgrid turbulence scheme based on Smagorinsky (1963) with modifications based on Lilly (1962) and Hill (1974), the LEAF-3 surface flux scheme (Walko et al. 2000), and the Harrington (1997) radiation scheme were employed. Longwave and shortwave radiation were sensitive to hydrometeors but not aerosol particles. Random perturbations to the ice–liquid potential temperature field were applied throughout the domain to initialize motions. The maximum magnitude of these perturbations was 0.1 K.

The simulations employed the Hebrew University spectral bin scheme (Khain et al. 2004), which has recently been interfaced with the RAMS dynamical core. All ice processes were turned off since only warm phase clouds were being simulated. The aerosol particles were

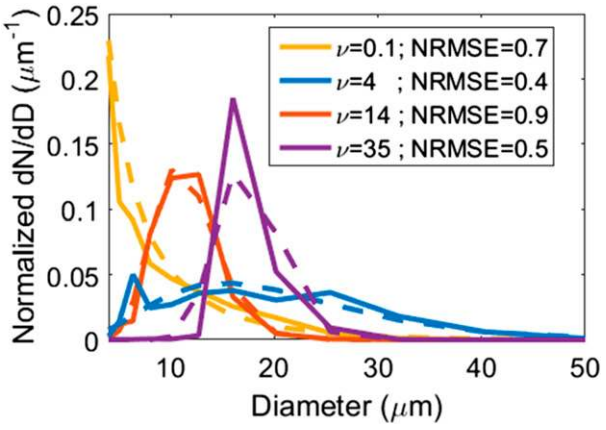

FIG. 2. Example simulated cloud droplet size distributions (solid lines) and the corresponding best-fit gamma distribution functions (dashed lines). The legend indicates the value of the best-fit shape parameter and the normalized root-mean-square error.

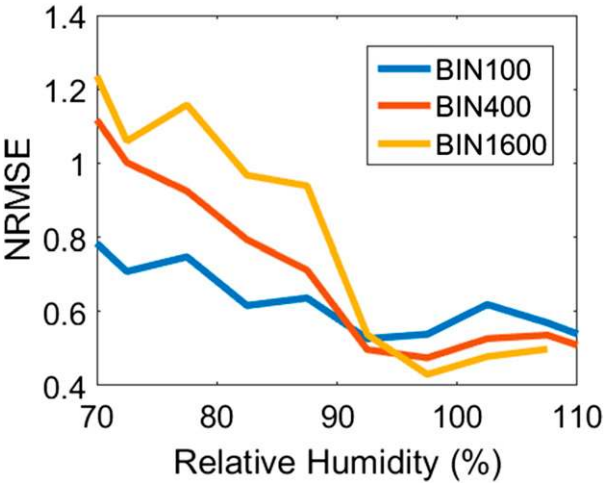

FIG. 3. Normalized root-mean-square error as a function of relative humidity for each simulation.

depleted upon cloud droplet nucleation. Droplet nucleation in the spectral bin scheme is performed by calculating a critical aerosol radius for activation based on Kohler theory (Khain et al. 2004). All aerosol particles larger than this critical size are activated to form new cloud droplets. No other aerosol processes were included in order to keep the aerosol physics as similar as possible between the Hebrew University spectral bin microphysics schemes and the RAMS bulk scheme (used in Part II).

Three simulations were run using a horizontally and vertically homogeneous aerosol concentration of 100, 400, or 1600 cm^{-3}. These concentrations are representative of clean, moderate, and polluted concentrations of accumulation mode aerosol particles at the ARM SGP site, respectively (Sheridan et al. 2001). The simulations will be referred to as BIN100, BIN400, and BIN1600. Aerosol particles were assumed to have a lognormal size distribution with a median radius of 40 nm and a spectral width of 1.8. No other source of new particles was present in the simulations.

Clouds first appear after about 4.5 h of simulation (1600 LST) at which point the boundary layer has become well developed (Fig. 1, medium gray line). Since the cloud base and boundary layer height were continuously rising in these simulations, new aerosol particles were continually being entrained from the free troposphere into the boundary layer. Therefore, the aerosol particles did not become depleted too rapidly and the average cloud droplet concentrations were approximately constant in time 2 h after clouds first appear (not shown). All analysis was conducted using data from the last 4 h (1700–2100 local time) of the simulations. The first hour in which clouds appear is excluded since during this time the clouds are not yet fully developed.

3. Results

Gamma probability distribution functions were fit to the explicitly predicted cloud droplet distributions at every cloudy grid point (cloud mixing ratio $> 0.01\,\mathrm{g\,kg^{-1}}$) using maximum-likelihood estimation methods in order to obtain best-fit shape parameters for each cloudy grid point. Figure 2 shows some example fitted distributions and the simulated droplet size distributions. These examples were chosen to illustrate that the method works well and to show that higher shape parameters correspond to relatively narrower droplet size distributions. By "relatively narrower" we mean the width scaled by the mean diameter decreases for higher shape parameters. To quantitatively determine how well the fitting performed, we calculated the normalized root-mean-square error (NRMSE). A value of 0 would indicate a perfect fit and a value of 1 indicates that the fitted PDF is no better than a straight line at approximating the simulated size distribution. The example simulated distributions in Fig. 2 have a range of NRMSEs in order to give a qualitative sense of these values. The NRMSE was averaged in 5% relative humidity bins and is shown in Fig. 3. The average NRMSE for relative humidity greater than about 90% is near 0.5 and indicates that the fitting generally performs well. Below 90%, the NRMSE increases rapidly, particularly for BIN1600. This result suggests that gamma distributions may not be appropriate for droplet distributions that are nearly evaporated.

Cross sections through two simulated cumulus clouds are shown in Fig. 4 from BIN100. The left side of the figure shows cross sections of cloud water mixing ratio, the center shows the corresponding droplet number concentration, and the right side of the figure shows the best-fit shape parameters for the cloud droplet size distributions. It can be seen that in general the highest shape

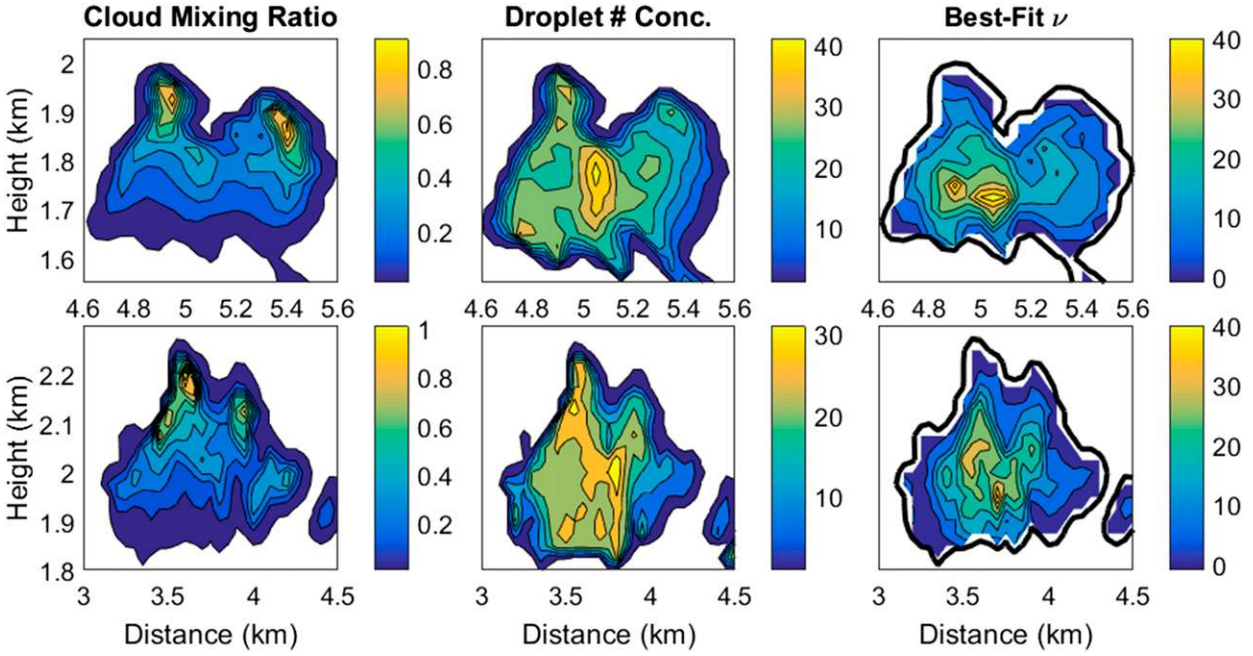

FIG. 4. Example cross sections of two different cumulus clouds. (left) The cloud mixing ratio (g kg^{-1}), (center) the droplet number concentration (mg^{-1}), and (right) the best-fit shape parameter are shown.

parameter values occur in the center of the cloud and that lower shape parameters are found along the cloud edges and at the cloud top. There is no obvious correlation between the shape parameter and the cloud mixing ratio, but there is a suggestion that there may be a correlation between the shape parameter and the droplet number concentration. In the upcoming discussion, we will explore the relationships between the best-fit shape parameters and cloud and environmental properties.

a. Shape parameter distributions

Frequency distributions of the best-fit shape parameters for all three simulations are shown in Fig. 5 in the solid lines. The average value of the best-fit shape parameter for all three simulations is about 5, which is a moderate value in comparison to the observationally obtained values listed in Table 1. While the average for each simulation is approximately the same, there is a clear shift to less frequent low values (except for the very lowest values) and more frequent high values of the shape parameter as the aerosol concentration is increased. This shift in frequency will be discussed more below.

The frequency distributions of the shape parameters also shift when they are separated into subsaturated and supersaturated regions (Fig. 5, dotted–dashed and dashed lines, respectively). In supersaturated regions, the average best-fit shape parameter increases to about 7 and the distribution of best-fit shape parameter values is broader, whereas in subsaturated regions it decreases to about 4 and the distribution of best-fit shape parameter values is much narrower. These results are consistent with past theoretical studies that have shown that the shape parameter (relative dispersion) should increase (decrease) during condensation, and vice versa during evaporation (Yum and Hudson 2005; Liu et al. 2006; Peng et al. 2007; Hsieh et al. 2009b; Wang et al. 2011; Pinsky et al. 2014). Additionally, lower values of the shape parameter are expected when entrainment and mixing are strong (Lu and Seinfeld 2006), and in these shallow cumulus clouds mixing should be stronger in the subsaturated areas along cloud edges rather than in the supersaturated areas located closer to the cloud center. Thus, both entrainment and evaporation work in concert to cause lower average shape parameters in subsaturated regions.

b. Dependence on relative humidity and vertical velocity

It is difficult to determine the relative importance of mixing/entrainment and condensation/evaporation for the cloud droplet distribution width. In an attempt to address this issue, the average shape parameter as a function of vertical velocity and relative humidity is plotted in Fig. 6 for BIN400. The corresponding figures for BIN100 and BIN1600 are qualitatively similar as that for BIN400 (not shown). The figure is broken into four quadrants. Points with positive vertical velocity and supersaturation likely occur in cloud cores where

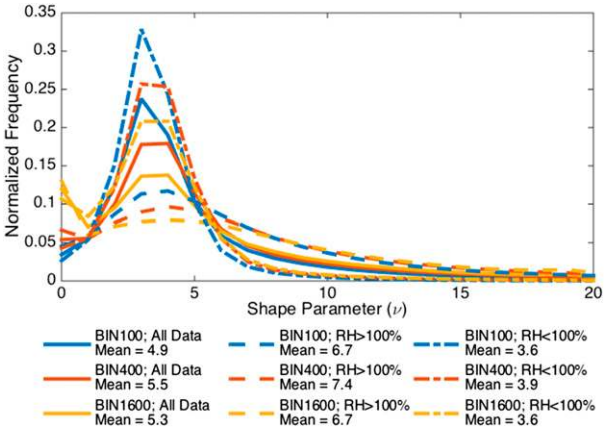

FIG. 5. Frequency distributions of the best-fit shape parameters. Frequency distributions from BIN100, BIN400, and BIN1600 are shown in blue, red, and yellow, respectively. The different line styles show the distribution using all data (solid), data from supersaturated regions (dashed), and data from subsaturated regions (dotted–dashed).

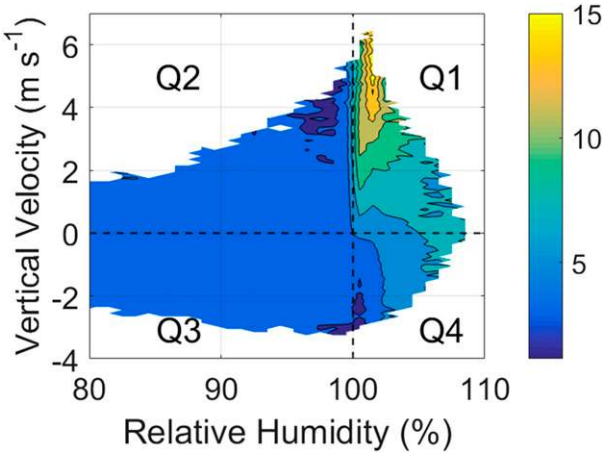

FIG. 6. Mean shape parameter as a function of relative humidity and vertical velocity from BIN400. Contours have an interval of 2 and begin at 1. Joint frequency bins with <10 data points have been excluded.

condensation rates are potentially high and mixing and entrainment are low (Q1; 35% of data points). Points with positive vertical velocity and subsaturation occur preferentially near cloud top where mixing and entrainment have just begun (Q2; 21% of data points). Points with negative vertical velocity are more likely to occur near cloud edges, with supersaturated points (Q4; 12% of data points) likely occurring closer to the cloud core and being less mixed than subsaturated points (Q3; 32% of data points). The most negative velocities occur where evaporation has been occurring for a long time and tend to occur along cloud edges near cloud base after having descended from above.

In agreement with the observations in shallow cumulus clouds, Fig. 6 shows that the highest shape parameters (lowest relative dispersions) occur in unmixed updrafts (Politovich 1993) in Q1. This is consistent with Fig. 4, which shows that the highest shape parameter values occur near the middle of the clouds. Concurrent entrainment of dry air and evaporation near cloud top in Q2 result in a rapid decrease of the shape parameter and cause some of the lowest shape parameters (highest relative dispersions) anywhere on Fig. 6. Such a rapid decrease near cloud top is consistent with previous modeling studies (Lu and Seinfeld 2006; Tas et al. 2012) and a theoretical study of homogeneous mixing (Pinsky et al. 2016). The other minimum in the average shape parameter occurs for the strongest downdrafts on the border of Q3 and Q4 where it is likely that sustained evaporation promotes the strong downdrafts and keeps the relative humidity near 100%. Again, these results are qualitatively consistent with Fig. 4, where it can be seen that the lowest shape parameter values occur along the cloud top and cloud edges. In the transition from Q1 to Q4 in which the air is always supersaturated, condensational growth tends to increase the shape parameter while mixing tends to decrease it. Entrainment and mixing are dominant and the shape parameter decreases as one moves from Q1 to Q4, but the transition is slow, especially compared to the transition between Q1 and Q2. From Q4 to Q3 (from supersaturated to subsaturated downdrafts) there is almost no discernible change, which indicates that condensation/evaporation has little impact and that entrainment and mixing are dominant. Overall, Fig. 6 seems to indicate that both entrainment/mixing and condensation/evaporation can both be strong controls on the shape parameter depending on the region of the cloud.

c. *Dependence on number concentration*

Figure 5 lists the average value of the shape parameter for each simulation in the legend. There is a nonmonotonic, but overall small change in the average best-fit shape parameter as the initial aerosol concentration increases. Examination of the shape parameter frequency distributions in Fig. 5 (solid lines) shows however that the mean is perhaps misleading. As the aerosol concentration increases, there is a shift to more frequent high values of the shape parameter and less frequent moderate values.

The primarily reason for this shift in shape parameter frequency is likely related to a decrease in cloud fraction with higher aerosol concentration (not shown, but discussed in Part II for bulk microphysics simulations with the same model setup). The reduced cloud fraction, which arises as a result of faster evaporation of the cloud

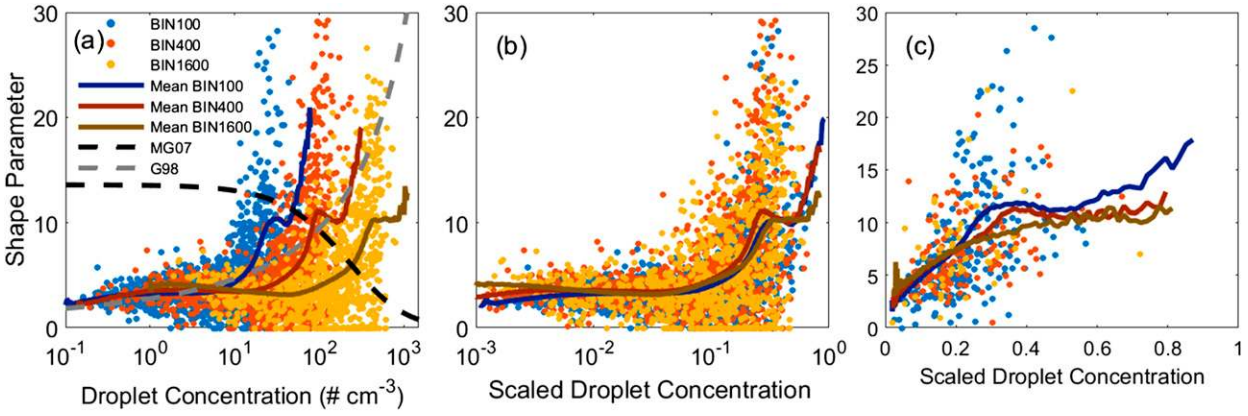

FIG. 7. (a) Points show the best-fit shape parameter value and droplet concentration of every two-thousandth cloudy point in each BIN simulation. Colored solid lines show the mean shape parameter as a function of the droplet concentration based on all cloudy points from each BIN simulation. Dashed gray lines show previously proposed relationships between the shape parameter and the droplet concentration. (b) As in (a), but the abscissa shows the droplet concentration normalized by the maximum droplet number concentration of each simulation (100, 400, or 1600 cm^{-3}). (c) As in (b), but for only those cloudy points with RH > 101% and $w > 0.1\ \mathrm{m\ s}^{-1}$ and every one-thousandth point is shown.

edges, is associated with a reduction in subsaturated cloudy volume fraction and an increase in the supersaturated cloudy volume fraction. This reduction in the subsaturated cloudy volume, which is associated with shape parameters of about 4 on average (Figs. 5 and 6), explains why we see a reduction in the normalized frequency of low shape parameters [~(1–5)] and an increase in the normalized frequency of high shape parameters (>5) for increasing aerosol concentration that was noted in Fig. 5.

The more frequent occurrence of shape parameters less than 1 as the aerosol concentration increases (Fig. 5) is more difficult to explain. These distributions with very low shape parameters appear more like exponential distributions (Fig. 2) and are associated with a large number of droplets in the very smallest size bin (which are likely to be freshly nucleated cloud droplets) that create a steep slope in the size distribution curve. With more droplets in the very smallest size bin, the steeper this slope and the lower the shape parameter. It is perhaps then not too surprising that these distributions are most frequent in the simulation with the highest aerosol concentration. It is the increase in both these lowest shape parameters and the increase in the highest shape parameters that works to keep the average shape parameter similar in all three simulations.

If there is in fact no dependence of the shape parameter on the aerosol concentration (or the cloud droplet concentration) in the mean, it may explain why previously reported values of the shape parameter from observations of shallow cumulus clouds do not consistently show either an increase or a decrease in shape parameter with aerosol concentration (Miles et al. 2000). Other factors, such as the width of the aerosol distribution, which was initially the same in all of the BIN simulations, or collision–coalescence in clouds that are more favorable for precipitation, may be important for determining whether the best-fit shape parameter increases or decreases as the aerosol concentration and cloud droplet concentration increase. Such factors have not been tested here.

While on average the shape parameter does not show a dependency on the initial aerosol concentration or mean droplet number concentration, the shape parameter does vary with the local droplet number concentration (Fig. 7a). For all three simulations, there is relatively little spread in the shape parameter values and little dependence on the cloud droplet number concentration when the cloud droplet number concentration is low. However, as the cloud droplet number concentration increases, the spread of shape parameter values becomes larger and the mean shape parameter increases. These trends are consistent with Figs. 5 and 6—high (low) droplet concentrations are more likely to be associated with the supersaturated (subsaturated) regions of clouds where it was found that the shape parameter is on average higher (lower) and the spread of values is also larger (smaller). These trends are also consistent with the fact that the condensation process tends to make distributions relatively narrower (favors high shape parameters) and vice versa for evaporation.

The qualitative relationship between the shape parameter and the droplet concentration is consistent across all three BIN simulations shown in Fig. 7a. Furthermore, when the droplet number concentration is scaled by the maximum cloud droplet concentration (Fig. 7b), the relationships between the scaled droplet concentration and the shape parameter for each simulation become nearly identical. This implies that for these simulations of nonprecipitating cumulus clouds, there is only a minimal

influence of the mean droplet concentration on the mean relationship between the local values of the shape parameter and the droplet concentration. (It is not obvious though whether this result can be applied to other cloud types or even precipitating cumulus clouds since the precipitation process is also expected to influence the relative dispersion of the droplet size distribution.) Thus, while the mean shape parameter associated with each simulation is not strongly dependent on the mean aerosol or droplet concentration (Fig. 5), there is a strong relationship between the local values of the shape parameter and the local values of the droplet number concentration (Fig. 7). Differing trends in cloud-averaged and local values have also been found in observations of continental cumulus clouds (Lu et al. 2012) and stratocumulus clouds (Pawlowska et al. 2006).

Again, the theoretical work that focuses on the condensation process shows that we expect a lower shape parameter (higher relative dispersion) for a higher aerosol concentration (Yum and Hudson 2005; Liu et al. 2006; Peng et al. 2007; Pinsky et al. 2014). While we do not see such a relationship in Figs. 5 and 7b when looking at all cloudy points, we do see this expected relationship for those cloudy points that are highly supersaturated and located within updrafts. Figures 7c is similar to Fig. 7b but uses only those cloudy points that have a relative humidity $\geq 101\%$ and vertical velocity $\geq 0.1\,\mathrm{m\,s^{-1}}$. For a scaled droplet concentration greater than about 0.2, there is a monotonic decrease in the average shape parameter as the initial aerosol concentration increases. Thus, the shallow cumulus clouds do have the expected relationship between aerosol concentration and mean shape parameter where condensation is strong, but other processes—such as evaporation, entrainment, and mixing, which were generally not considered in the parcel modeling and theoretical studies (Yum and Hudson 2005; Liu et al. 2006; Peng et al. 2007; Pinsky et al. 2014)—obscure this relationship when looking at all cloudy points. More investigation of how these other processes impact the relationship between aerosol concentration and the shape parameter or relative dispersion is needed.

d. Implication for parameterizations

Most papers in the literature that examine the relationship between the shape parameter and the droplet number concentration discuss how the average droplet concentration of a cloud relates to the average shape parameter of the cloud. However, Fig. 7 shows that even if there is no correlation between the cloud-averaged shape parameter and cloud-averaged droplet concentration, there can still be a strong correlation between the local values of these quantities within clouds.

One important implication of this distinction applies to model parameterizations for the shape parameter. Most parameterizations of the shape parameter have been developed to actively diagnose the most appropriate value of the shape parameter at each grid point during run time based on the relationship derived from cloud-averaged values. One example is the proposed relationship from Morrison and Grabowski (2007), which is shown by the black dashed line in Fig. 7a. This parameterization, among others (Rotstayn and Liu 2003; Thompson and Eidhammer 2014), prescribes a negative correlation between the droplet concentration and the shape parameter. This may be a reasonable relationship based on previous work looking at cloud-averaged values. However, given the physical reasoning discussed above and the support of this reasoning based on observations and theoretical work, it is probably unreasonable to expect that these relationships even qualitatively describe the relationship between the local values of the shape parameter and droplet concentrations within clouds. Instead, it appears that parameterizations such as the one proposed by Grabowski (1998) (dashed gray line in Fig. 7a) are more suitable for large-eddy simulations. (Recall that our grid spacing is $50\,\mathrm{m} \times 50\,\mathrm{m} \times 25\,\mathrm{m}$.) Also, note that in the BIN simulations, collision–coalescence was minimal and it is unclear how large its impact on these relationships could be.

Finally, it should be noted that the average value of the best-fit shape parameter is highly dependent on the averaging area. For the results shown in this paper, shape parameters were calculated at every cloudy grid point. If, however, the size distributions are averaged over multiple grid points before fitting, extreme values become less frequent, and the average itself decreases to lower values (not shown). Miles et al. (2000) presented similar findings pertaining to observational analyses. This should be kept in mind when interpreting the results of this and other studies that examine the relative dispersion of hydrometeor distributions.

4. Conclusions

In this study, simulations of nonprecipitating shallow cumulus clouds over land have been conducted using the Hebrew University spectral bin scheme (Khain et al. 2004) within the RAMS dynamical framework. With these simulations, several relationships between the shape parameter/relative dispersion of cloud droplets and environmental and cloud properties have been explored.

Both observations and the bin simulations showed that a wide range of values are possible for the cloud droplet distribution shape parameter. The simulations revealed that the average shape parameter is highest in supersaturated updrafts and lowest in subsaturated regions of the cloud. Both condensation/evaporation and

entrainment/mixing appear to play important roles in determining the relative dispersion of the cloud droplet size distributions simulated by the spectral bin model in these nonprecipitating shallow cumulus clouds.

There has been some debate about what the dependence of the relative dispersion (and hence the gamma distribution shape parameter) is on the cloud droplet number concentration (e.g., Miles et al. 2000; Liu and Daum 2002). The bin simulations do not indicate that there is any relationship between these two quantities when averaged over all clouds. While the initial studies on this topic promoted the idea that the shape parameter (relative dispersion) of cloud droplet size distributions decreases (increases) with cloud droplet concentration (Martin et al. 1994; Costa et al. 2000; Liu and Daum 2002), there is increasing evidence (Miles et al. 2000; Lu and Seinfeld 2006; Hsieh et al. 2009b; Geoffroy et al. 2010), including this study, which suggests that this is not always the case. Specifically, when looking at all cloudy points, this study found no consistent increase or decrease in the mean shape parameter as the aerosol concentration, and hence mean droplet concentration, was increased. However, when we limited the analysis to cloudy points in supersaturated updrafts, we found that the mean shape parameter decreased as the aerosol concentration increased, consistent with theoretical expectations.

Nonetheless, within individual clouds, there was a positive correlation between local values of the shape parameter and the cloud droplet number concentration, particularly in supersaturated regions of the clouds. This result highlights the fact that different relationships between the shape parameter and droplet concentration may exist depending on whether one looks at local or cloud-averaged values. Furthermore, it suggests that previous parameterizations for the cloud droplet shape parameter that were developed based on cloud-averaged values may be inappropriate.

It is unclear how the results discussed here may change for other warm phase cloud types or how the presence of active collision–coalescence would change the results. Additionally, these simulations have neglected aerosol regeneration upon evaporation, and this process may be important for shallow cumulus clouds. These additional avenues of research should be addressed in future work.

Finally, note that while our analysis has been done in the framework of gamma distribution shape parameters due to the implications for bulk microphysics schemes, the shape parameter is directly related to the relative dispersion of any distribution. The relative dispersion is a general property of any distribution. Thus, our analysis is relevant to real clouds with droplet size distributions that may or may not closely conform to gamma distributions.

Acknowledgments. The authors thank Alexander Khain for providing his spectral bin microphysics code and three anonymous reviewers for their constructive comments. This material is based on work supported by the National Science Foundation Graduate Research Fellowship Program under Grant DGE-1321845 and the National Aeronautics and Space Administration Grant NNX13AQ32G.

REFERENCES

Cohen, C., and E. W. McCaul, 2006: The sensitivity of simulated convective storms to variations in prescribed single-moment microphysics parameters that describe particle distributions, sizes, and numbers. *Mon. Wea. Rev.*, **134**, 2547–2565, doi:10.1175/MWR3195.1.

Costa, A. A., C. J. De Oliveira, J. C. P. De Oliveira, and A. J. D. C. Sampaio, 2000: Microphysical observations of warm cumulus clouds in Ceara, Brazil. *Atmos. Res.*, **54**, 167–199, doi:10.1016/S0169-8095(00)00045-4.

Cotton, W. R., and Coauthors, 2003: RAMS 2001: Current status and future directions. *Meteor. Atmos. Phys.*, **82**, 5–29, doi:10.1007/s00703-001-0584-9.

Feingold, G., R. Boers, B. Stevens, and W. R. Cotton, 1997: A modeling study of the effect of drizzle on cloud optical depth and susceptibility. *J. Geophys. Res.*, **102**, 13 527–13 534, doi:10.1029/97JD00963.

Geoffroy, O., J.-L. Brenguier, and F. Burnet, 2010: Parametric representation of the cloud droplet spectra for LES warm bulk microphysical schemes. *Atmos. Chem. Phys.*, **10**, 4835–4848, doi:10.5194/acp-10-4835-2010.

Gonçalves, F. L. T., J. A. Martins, and M. A. Silva Dias, 2008: Shape parameter analysis using cloud spectra and gamma functions in the numerical modeling RAMS during LBA Project at Amazonian region, Brazil. *Atmos. Res.*, **89**, 1–11, doi:10.1016/j.atmosres.2007.12.005.

Grabowski, W. W., 1998: Toward cloud resolving modeling of large-scale tropical circulations: A simple cloud microphysics parameterization. *J. Atmos. Sci.*, **55**, 3283–3298, doi:10.1175/1520-0469(1998)055<3283:TCRMOL>2.0.CO;2.

Harrington, J. Y., 1997: The effects of radiative and microphysical processes on simulation of warm and transition season Arctic stratus. Ph.D. dissertation, Colorado State University, 289 pp. [Available online at http://www.personal.psu.edu/users/m/r/mrh318/Harrington-CSU-1997.pdf.]

Hill, G. E., 1974: Factors controlling the size and spacing of cumulus clouds as revealed by numerical experiments. *J. Atmos. Sci.*, **31**, 646–673, doi:10.1175/1520-0469(1974)031<0646:FCTSAS>2.0.CO;2.

Hsieh, W. C., H. Jonsson, L.-P. Wang, G. Buzorius, R. C. Flagan, J. H. Seinfeld, and A. Nenes, 2009a: On the representation of droplet coalescence and autoconversion: Evaluation using ambient cloud droplet size distributions. *J. Geophys. Res.*, **114**, D07201, doi:10.1029/2008JD010502.

——, A. Nenes, R. C. Flagan, J. H. Seinfeld, G. Buzorius, and H. Jonsson, 2009b: Parameterization of cloud droplet size distributions: Comparison with parcel models and observations. *J. Geophys. Res.*, **114**, D11205, doi:10.1029/2008JD011387.

Hudson, J. G., S. Noble, and V. Jha, 2012: Cloud droplet spectral width relationship to CCN spectra and vertical velocity. *J. Geophys. Res.*, **117**, D11211, doi:10.1029/2012JD017546.

Igel, A. L., and S. C. van den Heever, 2016: The importance of the shape of cloud droplet size distributions in shallow cumulus clouds. Part II: Bulk microphysics simulations. *J. Atmos. Sci.*, **74**, 259–273, doi:10.1175/JAS-D-15-0383.1.

Khain, A., A. Pokrovsky, M. Pinsky, A. Seifert, and V. Phillips, 2004: Simulation of effects of atmospheric aerosols on deep turbulent convective clouds using a spectral microphysics mixed-phase cumulus cloud model. Part I: Model description and possible applications. *J. Atmos. Sci.*, **61**, 2963–2982, doi:10.1175/JAS-3350.1.

——, and Coauthors, 2015: Representation of microphysical processes in cloud-resolving models: Spectral (bin) microphysics versus bulk parameterization. *Rev. Geophys.*, **53**, 247–322, doi:10.1002/2014RG000468.

Lilly, D. K., 1962: On the numerical simulation of buoyant convection. *Tellus*, **14**, 148–172, doi:10.1111/j.2153-3490.1962.tb00128.x.

Liu, Y., and P. H. Daum, 2002: Anthropogenic aerosols: Indirect warming effect from dispersion forcing. *Nature*, **419**, 580–581, doi:10.1038/419580a.

——, ——, and S. S. Yum, 2006: Analytical expression for the relative dispersion of the cloud droplet size distribution. *Geophys. Res. Lett.*, **33**, L02810, doi:10.1029/2005GL024052.

Loftus, A. M., and W. R. Cotton, 2014: Examination of CCN impacts on hail in a simulated supercell storm with triple-moment hail bulk microphysics. *Atmos. Res.*, **147–148**, 183–204, doi:10.1016/j.atmosres.2014.04.017.

Lu, M.-L., and J. H. Seinfeld, 2006: Effect of aerosol number concentration on cloud droplet dispersion: A large-eddy simulation study and implications for aerosol indirect forcing. *J. Geophys. Res.*, **111**, D02207, doi:10.1029/2005JD006419.

——, G. Feingold, H. H. Jonsson, P. Y. Chuang, H. Gates, R. C. Flagan, and J. H. Seinfeld, 2008: Aerosol-cloud relationships in continental shallow cumulus. *J. Geophys. Res.*, **113**, D15201, doi:10.1029/2007JD009354.

Lu, C., Y. Liu, S. Niu, and A. M. Vogelmann, 2012: Observed impacts of vertical velocity on cloud microphysics and implications for aerosol indirect effects. *Geophys. Res. Lett.*, **39**, L21808, doi:10.1029/2012GL053599.

Martin, G. M., D. W. Johnson, and A. Spice, 1994: The measurement and parameterization of effective radius of droplets in warm stratocumulus clouds. *J. Atmos. Sci.*, **51**, 1823–1842, doi:10.1175/1520-0469(1994)051<1823:TMAPOE>2.0.CO;2.

Martins, J. A., and M. A. F. Silva Dias, 2009: The impact of smoke from forest fires on the spectral dispersion of cloud droplet size distributions in the Amazonian region. *Environ. Res. Lett.*, **4**, 015002, doi:10.1088/1748-9326/4/1/015002.

Milbrandt, J. A., and M. K. Yau, 2005a: A multimoment bulk microphysics parameterization. Part I: Analysis of the role of the spectral shape parameter. *J. Atmos. Sci.*, **62**, 3051–3064, doi:10.1175/JAS3534.1.

——, and ——, 2005b: A multimoment bulk microphysics parameterization. Part II: A proposed three-moment closure and scheme description. *J. Atmos. Sci.*, **62**, 3065–3081, doi:10.1175/JAS3535.1.

Miles, N. L., J. Verlinde, and E. E. Clothiaux, 2000: Cloud droplet size distributions in low-level stratiform clouds. *J. Atmos. Sci.*, **57**, 295–311, doi:10.1175/1520-0469(2000)057<0295:CDSDIL>2.0.CO;2.

Morrison, H., and W. W. Grabowski, 2007: Comparison of bulk and bin warm-rain microphysics models using a kinematic framework. *J. Atmos. Sci.*, **64**, 2839–2861, doi:10.1175/JAS3980.

Paluch, I. R., and D. G. Baumgardner, 1989: Entrainment and fine-scale mixing in a continental convective cloud. *J. Atmos. Sci.*, **46**, 261–278, doi:10.1175/1520-0469(1989)046<0261:EAFSMI>2.0.CO;2.

Pandithurai, G., S. Dipu, T. V. Prabha, R. S. Maheskumar, J. R. Kulkarni, and B. N. Goswami, 2012: Aerosol effect on droplet spectral dispersion in warm continental cumuli. *J. Geophys. Res.*, **117**, D16202, doi:10.1029/2011JD016532.

Pawlowska, H., W. W. Grabowski, and J.-L. Brenguier, 2006: Observations of the width of cloud droplet spectra in stratocumulus. *Geophys. Res. Lett.*, **33**, L19810, doi:10.1029/2006GL026841.

Peng, Y., U. Lohmann, R. Leaitch, and M. Kulmala, 2007: An investigation into the aerosol dispersion effect through the activation process in marine stratus clouds. *J. Geophys. Res.*, **112**, D11117, doi:10.1029/2006JD007401.

Pinsky, M., I. P. Mazin, A. Korolev, and A. Khain, 2014: Supersaturation and diffusional droplet growth in liquid clouds: Polydisperse spectra. *J. Geophys. Res. Atmos.*, **119**, 12 872–12 887, doi:10.1002/2014JD021885.

——, A. Khain, A. Korolev, and L. Magaritz-Ronen, 2016: Theoretical investigation of mixing in warm clouds—Part 2: Homogeneous mixing. *Atmos. Chem. Phys.*, **16**, 9255–9272, doi:10.5194/acp-16-9255-2016.

Politovich, M. K., 1993: A study of the broadening of droplet size distributions in cumuli. *J. Atmos. Sci.*, **50**, 2230–2244, doi:10.1175/1520-0469(1993)050<2230:ASOTBO>2.0.CO;2.

Rotstayn, L. D., and Y. Liu, 2003: Sensitivity of the first indirect aerosol effect to an increase of cloud droplet spectral dispersion with droplet number concentration. *J. Climate*, **16**, 3476–3481, doi:10.1175/1520-0442(2003)016<3476:SOTFIA>2.0.CO;2.

Sheridan, P. J., D. J. Delene, and J. A. Ogren, 2001: Four years of continuous surface aerosol measurements from the Department of Energy's Atmospheric Radiation Measurement Program Southern Great Plains Cloud and Radiation Testbed site. *J. Geophys. Res.*, **106**, 20 735–20 747, doi:10.1029/2001JD000785.

Shipway, B. J., and A. A. Hill, 2012: Diagnosis of systematic differences between multiple parametrizations of warm rain microphysics using a kinematic framework. *Quart. J. Roy. Meteor. Soc.*, **138**, 2196–2211, doi:10.1002/qj.1913.

Smagorinsky, J., 1963: General circulation experiments with the primitive equations. *Mon. Wea. Rev.*, **91**, 99–164, doi:10.1175/1520-0493(1963)091<0099:GCEWTP>2.3.CO;2.

Tas, E., I. Koren, and O. Altaratz, 2012: On the sensitivity of droplet size relative dispersion to warm cumulus cloud evolution. *Geophys. Res. Lett.*, **39**, L13807, doi:10.1029/2012GL052157.

Thompson, G., and T. Eidhammer, 2014: A study of aerosol impacts on clouds and precipitation development in a large winter cyclone. *J. Atmos. Sci.*, **71**, 3636–3658, doi:10.1175/JAS-D-13-0305.1.

——, P. R. Field, W. D. Hall, and R. M. Rasmussen, 2008: Explicit forecasts of winter precipitation using an improved bulk microphysics scheme. Part II: Implementation of a new snow parameterization. *Mon. Wea. Rev.*, **136**, 5095–5115, doi:10.1175/2008MWR2387.1.

Walko, R. L., W. R. Cotton, M. P. Meyers, and J. Y. Harrington, 1995: New RAMS cloud microphysics parameterization part I: The single-moment scheme. *Atmos. Res.*, **38**, 29–62, doi:10.1016/0169-8095(94)00087-T.

——, and Coauthors, 2000: Coupled atmosphere–biophysics–hydrology models for environmental modeling. *J. Appl. Meteor.*, **39**, 931–944, doi:10.1175/1520-0450(2000)039<0931:CABHMF>2.0.CO;2.

Wang, X., H. Xue, W. Fang, and G. Zheng, 2011: A study of shallow cumulus cloud droplet dispersion by large eddy simulations. *Acta Meteor. Sin.*, **25**, 166–175, doi:10.1007/s13351-011-0024-9.

Yum, S. S., and J. G. Hudson, 2005: Adiabatic predictions and observations of cloud droplet spectral broadness. *Atmos. Res.*, **73**, 203–223, doi:10.1016/j.atmosres.2004.10.006.

Zhu, P., and B. Albrecht, 2003: Large eddy simulations of continental shallow cumulus convection. *J. Geophys. Res.*, **108**, 4453, doi:10.1029/2002JD003119.